Journal of Applied Physics

Temperature dependent elastic constants and thermodynamic properties of BAs: An *ab initio* investigation

Cite as: J. Appl. Phys. **127**, 245103 (2020); https://doi.org/10.1063/5.0011111
Submitted: 17 April 2020 . Accepted: 04 June 2020 . Published Online: 22 June 2020

Cristiano Malica, and Andrea Dal Corso

AIP Publishing

Journal of Applied Physics ARTICLE scitation.org/journal/jap

Temperature dependent elastic constants and thermodynamic properties of BAs: An *ab initio* investigation

Cite as: J. Appl. Phys. **127**, 245103 (2020); doi: 10.1063/5.0011111
Submitted: 17 April 2020 · Accepted: 4 June 2020 ·
Published Online: 22 June 2020

Cristiano Malica[1,a] and Andrea Dal Corso[1,2]

AFFILIATIONS

[1]International School for Advanced Studies (SISSA), Via Bonomea 265, 34136 Trieste, Italy
[2]IOM-CNR, 34136 Trieste, Italy

[a]**Author to whom correspondence should be addressed:** cmalica@sissa.it

ABSTRACT

We present an *ab initio* study of the temperature dependent elastic constants of boron arsenide, a semiconductor that exhibits ultra-high thermal conductivity and is under investigation for thermal management in electronics. We test the consistency of our predictions by computing the temperature dependent sound velocity of the longitudinal acoustic mode along the [111] direction and comparing with experiments. Furthermore, as a by-product, we present the room temperature phonon dispersions and the temperature dependent thermal expansion, isobaric heat capacity, and average Grüneisen parameter compared with the most updated experiments and previous calculations when available. Finally, we present the theoretical estimate of the temperature dependent mean square atomic displacements.

I. INTRODUCTION

Boron arsenide (BAs) is a promising semiconductor due to its high thermal conductivity at room temperature (RT) that makes it a possible candidate for applications in electronics and photonics that require efficient heat dissipation from hot spots in devices. Although the growth of BAs has been reported since 1950s, only recently high-quality samples have been synthesized with the measurement of an ultrahigh thermal conductivity up to $1300\,\mathrm{W\,m^{-1}\,K^{-1}}$.[1–4] These measurements spurred the interest for this material so that many experiments and theoretical calculations have been carried out to investigate its physical properties. BAs has a zinc-blende cubic structure and belongs to the space group $F\bar{4}3m$.[2–4] Recent measurements, supported by *ab initio* calculations, range from the lattice constant and thermal expansion (TE), to the bandgap and refractive index, to the elastic constants (ECs) and the bulk modulus.[5–7]

The ECs are important quantities to describe the mechanical and thermodynamic properties of materials since they allow us to check the crystal stability, determine the speeds of sound, and can be used to compute the TE and the thermal stresses. At $T = 0\,\mathrm{K}$, the ECs of BAs have been computed in several works by means of density functional theory (DFT) using several exchange and correlation functionals.[5,6,8–12] However, in the literature, the information about the effect of temperature on the ECs is rather indirect. Kang *et al.*[6] reported the measured speed of sound of the longitudinal acoustic mode along the [111] direction from $T = 80\,\mathrm{K}$ to $T = 500\,\mathrm{K}$, showing a decrease of about 2.4%, but no theoretical calculation is available to support this measurement and, in general, to estimate the temperature dependent elastic constants (TDECs) of BAs.

We have recently implemented in the thermo_pw code[13] the calculation of the TDECs, both isothermal and adiabatic. The TDECs can be computed from second derivatives of the Helmholtz free-energy within the quasi-harmonic approximation (QHA) by means of density functional theory (DFT) and density functional perturbation theory (DFPT). In this paper, we apply the calculation of TDECs to BAs. We found that in the temperature range $0-1800\,\mathrm{K}$, the percentage softening of adiabatic ECs is approximately 11% for C_{11}, approximately 9% for C_{12}, and approximately 13% for C_{44}. In the temperature range 0–800 K, the softening is comparable but slightly smaller than the one of silicon.

As a by-product of our calculation, we report the RT phonon dispersions of BAs compared with the inelastic x-ray scattering measurements and the temperature dependence of several other thermodynamic quantities such as the TE, the isobaric heat capacity, the average Grüneisen parameter, and the atomic B-factors

(BFs). We compare these quantities with experimental data and previous calculations when available. In general, the agreement is quite good.

II. THEORY

The calculation of the TDECs within the QHA has been explained in detail in our recent work;[13] in this section we limit ourselves to a summary of the most important formulas in order to make the paper self-contained.

The isothermal ECs are obtained from the derivatives of the Helmholtz free-energy F with respect to strain $\boldsymbol{\epsilon}$

$$\tilde{C}^T_{ijkl} = \frac{1}{\Omega}\left(\frac{\partial^2 F}{\partial \epsilon_{ij}\partial \epsilon_{kl}}\right)_{\epsilon=0}. \tag{1}$$

Since we are usually interested in the ECs obtained from the stress–strain relationship (C^T_{ijkl}), we correct the $\tilde{C}^T_{ijkl}$ when the system is under a pressure p as

$$C^T_{ijkl} = \tilde{C}^T_{ijkl} + \frac{1}{2}p\left(2\delta_{ij}\delta_{kl} - \delta_{il}\delta_{jk} - \delta_{ik}\delta_{jl}\right). \tag{2}$$

The Helmholtz free-energy of Eq. (1) is obtained as the sum of the DFT total energy U and the vibrational free-energy (neglecting the electronic contribution): $F = U + F_{vib}$. The latter is given by

$$F_{vib}(\boldsymbol{\epsilon}, \mathbf{T}) = \frac{1}{2N}\sum_{\mathbf{q}\eta}\hbar\omega_\eta(\mathbf{q}, \boldsymbol{\epsilon}) + \frac{k_B T}{N}\sum_{\mathbf{q}\eta}\ln\left[1 - \exp\left(-\frac{\hbar\omega_\eta(\mathbf{q}, \boldsymbol{\epsilon})}{k_B T}\right)\right], \tag{3}$$

where N is the number of cells in the crystal and $\omega_\eta(\mathbf{q}, \boldsymbol{\epsilon})$ is the phonon angular frequency of the mode η with wave-vector $\mathbf{q}$ computed in the system with a strain $\boldsymbol{\epsilon}$. Cubic solids have three independent ECs that in Voigt notations are C_{11}, C_{12}, and C_{44}.[14] The QHA calculation of the ECs, Eq. (1), is performed on a grid of reference geometries by varying the lattice constant a_0. Phonon dispersions are computed in the same grid in order to evaluate the free-energy as a function of the volume, minimize it, and obtain the temperature dependent crystal parameter $a(T)$.[15,16] Then, at each temperature T, the TDECs as a function of a_0 are interpolated and evaluated at $a(T)$. The calculation requires phonon dispersions in all the strained configurations for all the reference geometries, in addition to the phonon dispersions used to compute $a(T)$.

The temperature dependent lattice parameter $a(T)$ can be used to derive the TE α as

$$\alpha = \frac{1}{a(T)}\frac{da(T)}{dT}. \tag{4}$$

The isochoric heat capacity within the harmonic approximation is given by

$$C_V = \frac{k_B}{N}\sum_{\mathbf{q}\eta}\left(\frac{\hbar\omega_\eta(\mathbf{q})}{k_B T}\right)^2 \frac{\exp(\hbar\omega_\eta(\mathbf{q})/k_B T)}{[\exp(\hbar\omega_\eta(\mathbf{q})/k_B T) - 1]^2}. \tag{5}$$

It is computed for each reference geometry and it is interpolated at $a(T)$. The knowledge of α and C_V allows us to compute the isobaric heat capacity C_P and the average Grüneisen parameter γ,

$$C_P = C_V + T\Omega\beta^2 B^T, \tag{6}$$

$$\gamma = \frac{\Omega\beta B^T}{C_V}, \tag{7}$$

where Ω is the volume of one unit cell at the temperature T, $\beta = 3\alpha$ is the volume TE, and B^T is the isothermal bulk modulus calculated from the ECs as

$$B^T = \frac{1}{3}\left(C^T_{11} + 2C^T_{12}\right). \tag{8}$$

The adiabatic ECs C^S_{ijkl} are obtained from the isothermal ones with the relation

$$C^S_{ijkl} = C^T_{ijkl} + \frac{T\Omega b_{ij} b_{kl}}{C_V}, \tag{9}$$

where the b_{ij} are the thermal stresses obtained from

$$b_{ij} = -\sum_{kl} C^T_{ijkl}\alpha_{kl}. \tag{10}$$

The adiabatic bulk modulus B^S is computed as in Eq. (8) in terms of the adiabatic ECs.

The atomic BF is calculated as explained in a previous work.[17] Calling $B_{\alpha\beta}(s)$ the mean square displacement matrix of the atom s, we have

$$B_{\alpha\beta}(s) = \frac{\hbar}{2NM_s}\sum_{\mathbf{q}\eta}\coth\left[\frac{\hbar\,\omega_\eta(\mathbf{q})}{2k_B T}\right]\frac{u^\eta_{s\alpha}(\mathbf{q})\left[u^\eta_{s\beta}(\mathbf{q})\right]^*}{\omega_\eta(\mathbf{q})}, \tag{11}$$

where M_s is the mass of sth atom, $u^\eta_{s\alpha}(\mathbf{q})$ is the $s\alpha$th component of the dynamical matrix eigenvector of the mode η with wave-vector $\mathbf{q}$. The BF is defined as $8\pi^2 B_{\alpha\beta}(s)$.[17] In order to include anharmonic effects, BFs are computed in the same reference geometries used for elastic constants and interpolated at each temperature at the $a(T)$.

III. METHOD

The calculations presented in this work were carried out using DFT as implemented in the Quantum ESPRESSO package.[18,19] Thermodynamic properties have been computed using the thermo_pw package.[20] The exchange and correlation functional was approximated by the local density approximation (LDA), which gives the best agreement between experimental and theoretical quantities, especially for the $T = 0$ K ECs. We employed the projector augmented wave (PAW) method and a plane waves basis set with pseudopotentials[21] from *pslibrary*.[22] The pseudopotentials `B.pz-n-kjpaw_psl.1.0.0.UPF` and `As.pz-n-kjpaw_psl.1.0.0.UPF` have been used for boron

TABLE I. The computed ECs compared with some results available in the literature. The exchange and correlation functionals are indicated in the first column. The equilibrium lattice constant (a_0) is in Å, while the ECs and the bulk modulus are in kbar. The experimental values are at $T = 298$ K.

	a_0	C_{11}	C_{12}	C_{44}	B
LDA[a]	4.745	2897	768	1557	1477
LDA[b]	4.745	2897	768	1772	1477
LDA[c]	4.756	2828	759	1520	1449
LDA[d]	4.759	2807	754	1507	1438
LDA[6]	4.7444	2940	806	1770	1500
LDA[12]		3013	772	1639	1519
LDA[11]	4.779	2864	710	1575	1428
LDA[10]	4.743	2950	780	1770	1500
LDA[8]	4.721	2914	728	1579	1457
PBE[5]	4.817	2630	620	1430	1290
PBE[10]	4.812	2750	630	1500	1340
PBE[9]	4.784	2510	798	1270	1370
Expt.[6]	4.78	2850	795	1490	1480

[a]This work at $T = 0$ K.
[b]This work at $T = 0$ K with frozen ions.
[c]This work at $T = 0$ K + ZPE.
[d]This work at $T = 300$ K (adiabatic ECs).

and arsenic, respectively. The wave functions (charge density) were expanded in a plane waves basis with a kinetic energy cut-off of 60 Ry (400 Ry), and a $16 \times 16 \times 16$ mesh of **k**-points has been used for the Brillouin zone integration. Density functional perturbation theory (DFPT)[23,24] was used to calculate the dynamical matrices on a $4 \times 4 \times 4$ **q**-points grid. The dynamical matrices have been Fourier interpolated on a $200 \times 200 \times 200$ **q**-points mesh to evaluate the free-energy. The grid of the reference geometries was centered at the $T = 0$ K lattice constant reported in Table I. The number of reference geometries was nine with lattice constants separated from each other by $\Delta a = 0.05\, a.u.$. In the EC calculation, the number of strained configuration was six for each type of strain with an interval of strains between two strained geometries of 0.005. In total, we computed phonon dispersions for 162 geometries [in addition to the nine phonon dispersions used for the $a(T)$ calculation]. A second degree polynomial has been used to fit the energy (for the ECs at $T = 0$ K) or the free-energy (for the QHA TDECs) as a function of strain, while a fourth degree polynomial was used to fit at each temperature all the other quantities computed at the various reference geometries vs $a(T)$.

IV. APPLICATIONS

In Table I, we report the computed equilibrium lattice constant a_0 at $T = 0$ K both with and without the zero point energy (ZPE) and the RT value: the differences among them are of the order of hundredths of angstroms. The computed RT a_0 is in good agreement with the RT experiment[6] (the difference is smaller than approximately 0.02 Å). The comparison with other computed a_0 is also reported: the LDA values agree within approximately 1%. These small differences depend primarily on the computational parameters chosen for the calculation and on different pseudopotentials. The PBE (Perdew Burke Ernzerhof) values of a_0 are slightly larger than the LDA ones as usually found with the functionals that use the generalized gradient approximation (GGA).

In Table I, we report the calculated values of the elastic constants together with other theoretical estimates available in the literature and the experimental values. The LDA values are closer to experimental values, while the PBE calculations give smaller ECs, as usually found with the GGA functionals. At $T = 0$ K, the softening due to the ZPE is approximately 2.4% for C_{11}, approximately 1.2% for C_{12}, and approximately 2.4% in C_{44}. In our calculation, we relax the ionic positions for each strained configuration, so the ECs are relaxed-ions results. This is relevant only for C_{44}, while for C_{11} and C_{12}, the ionic positions are determined by symmetry. The frozen-ion results, obtained by a uniform strain of the atomic positions but no further relaxation, are also shown in Table I: C_{44} is approximately 14% larger than the relaxed-ions value. Our theoretical $T = 300$ K values are in good agreement with experiment: C_{11} is smaller of approximately 1.5%, C_{12} is smaller of approximately 5.1%, and C_{44} is larger of approximately 1%.

In Fig. 1, the TDECs and the bulk modulus are reported. The red lines are the adiabatic ECs (or bulk modulus), while the blue lines are the isothermal ECs. Evaluating the percentage softening of ECs due to temperature as

$$\frac{C_{ij}(T = 0\,\mathrm{K}) - C_{ij}(T = 1800\,\mathrm{K})}{C_{ij}(T = 0\,\mathrm{K})} \times 100, \tag{12}$$

where the ZPE is included in $C_{ij}(T = 0\mathrm{K})$ we find approximately 11% (adiabatic) and approximately 13% (isothermal) for C_{11}, approximately 9% (adiabatic) and approximately 15% (isothermal) for C_{12}, and approximately 13% for C_{44}.

As far as we know, presently no experimental measurement of the TDECs is available to compare directly with our result, but recently the temperature dependence of the longitudinal sound velocity along the [111] direction was measured until approximately 500 K.[6] Using the adiabatic TDECs and the density ρ this sound velocity can be written as[27]

$$V_{long} = \left(\frac{C_{11} + 2C_{12} + 4C_{44}}{3\rho}\right)^{\frac{1}{2}}, \tag{13}$$

and in Fig. 2, we compare our theoretical estimate with the experimental one. We take into account the temperature dependence of the density due to the TE effect. The use of a temperature independent density in Eq. (13) (for instance, the density at $T = 0$ K or $T = 300$ K) leads to an appreciably lower sound velocity above the RT (for instance, at $T = 1500$ K, the difference is approximately 90 m/s). The theoretical values of the sound velocity as a function of temperature is in reasonable agreement with the experimental one in the analyzed range, but the experimental slope of the curve at low temperatures is not reproduced. The comparison improves above RT. The difference between theory and experiment at RT (0.9%) is compatible with the errors in the elastic constants and in the density, while the difference at the lowest measured temperature (2.3%) is larger.

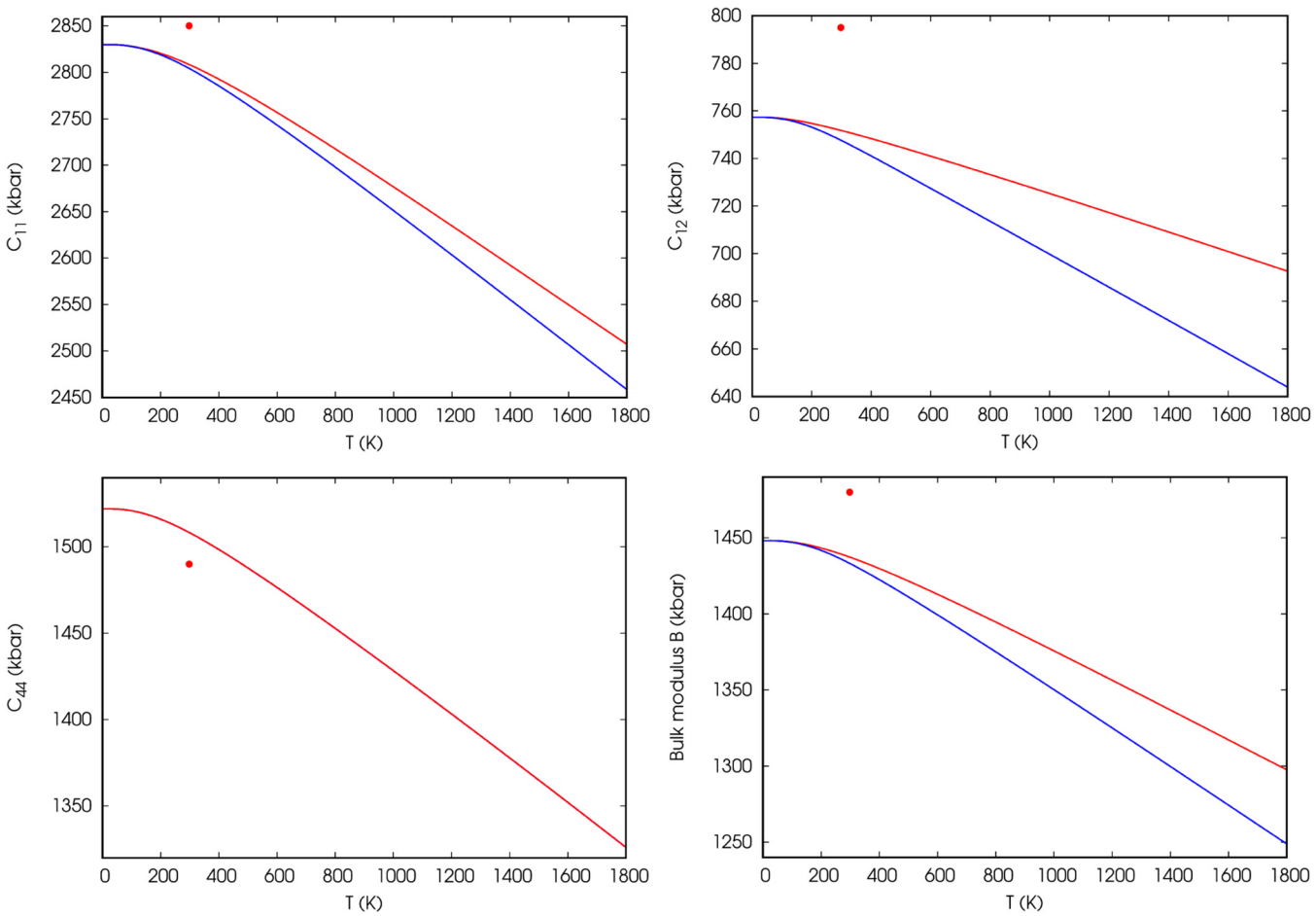

FIG. 1. TDECs and bulk modulus of BAs: isothermal (blue) and adiabatic (red). RT experimental points from Kang *et al.*[6]

We can also compare the TDECs of BAs with those of silicon that we have calculated by using LDA.[13] Silicon ECs are smaller, $T = 0$ K values (with ZPE) are $C_{11} = 1580$ kbar, $C_{12} = 639$ kbar, and $C_{44} = 746$ kbar. In the temperature range calculated for silicon (0−800 K), C_{11} and C_{12} decrease about 7% and C_{44} about 5% (for both isothermal and adiabatic). In the same temperature range, the decrease of the ECs of BAs is slightly smaller: 3.8% (adiabatic) and 4.5% (isothermal) for C_{11}, 3.2% (adiabatic) and 5.7% (isothermal) for C_{12}, and 4.5% for C_{44}.

We now present several other thermodynamic properties of BAs that have been calculated together with the TDECs. The TE and the temperature dependence of the lattice constant $a(T)$ are shown in Fig. 3 in the temperature range 0−1100 K. We compare our numerical result (black line) with two recent measurements in the temperature range 300−773 K (red points)[7] and 321–773 K (blue points).[6] The experimental $a(T)$ is higher than the theoretical one by approximately 0.02 Å, but the temperature dependence is reproduced correctly as visible in the TE plot reported in the same figure. In the experimental temperature range, the experimental $a(T)$ are both linear with T but the slope of the red points is slightly larger and

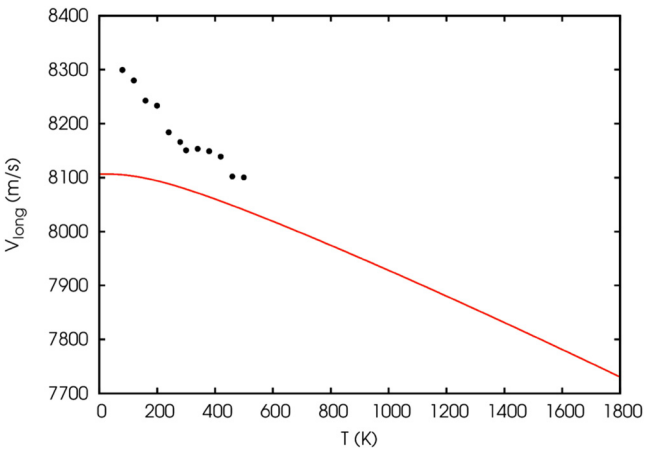

FIG. 2. Longitudinal sound velocity in the [111] direction: experimental points (extrapolated from Kang *et al.*[6]) and this work (red curve).

more in agreement with our calculation. This behavior is reflected in the TE: the TE of Chen *et al.*[7] agrees with ours within experimental uncertainties while the TE of Kang *et al.*[6] has slightly smaller values (although within the error bar of the former[7]). In particular, the RT TEs are $4.0 \times 10^{-6}\,\mathrm{K}^{-1}$ (this work), $(4.2 \pm 0.4) \times 10^{-6}\,\mathrm{K}^{-1}$ (Chen *et al.*[7]), and $3.85 \times 10^{-6}\,\mathrm{K}^{-1}$ (Kang *et al.*[6]). Other DFT-LDA estimates are $4.0 \times 10^{-6}\,\mathrm{K}^{-1}$ (Chen *et al.*[7]) and $3.04 \times 10^{-6}\,\mathrm{K}^{-1}$ (Broido *et al.*[28]). Molecular dynamic simulations[29] produced the result 4.1×10^{-6}. A much larger value has appeared recently[30] ($10.9 \times 10^{-6}\,\mathrm{K}^{-1}$) by using the DFT method within the GGA, quite far from experiment.

The phonon frequencies computed at the different geometries are interpolated at $T = 300$ K and the result is shown in Fig. 3(b) (colored lines). The phonons are compared with RT measurements obtained from inelastic x-ray scattering[25] and Raman spectroscopy[26] (points). As already found in previous Refs. 25 and 28, the agreement between theory and experiment is quite good. The difference between RT and $T = 0$ K phonons (black lines) is only barely visible in the optical branches.

The isobaric heat capacity is shown in Fig. 3(c). The points indicate the temperature dependence of experimental data below RT[7] that we extrapolated from the plot. The agreement is very good, consistent with the fact that also the calculated Debye temperature ($\Theta_D = 668$ K, obtained from the $T = 0$ K+ ZPE ECs) is in good agreement with the experimental value[7] ($\Theta_D = 681$ K).

The temperature dependence of the average Grüneisen parameter is reported in Fig. 3(d). We also report the RT experimental values of Kang *et al.*[6] (blue point) and Chen *et al.*[7] (orange point). The experimental uncertainty of the first point is not known, but it is very close to our curve. The second point is in agreement with our estimate within the experimental error bar.

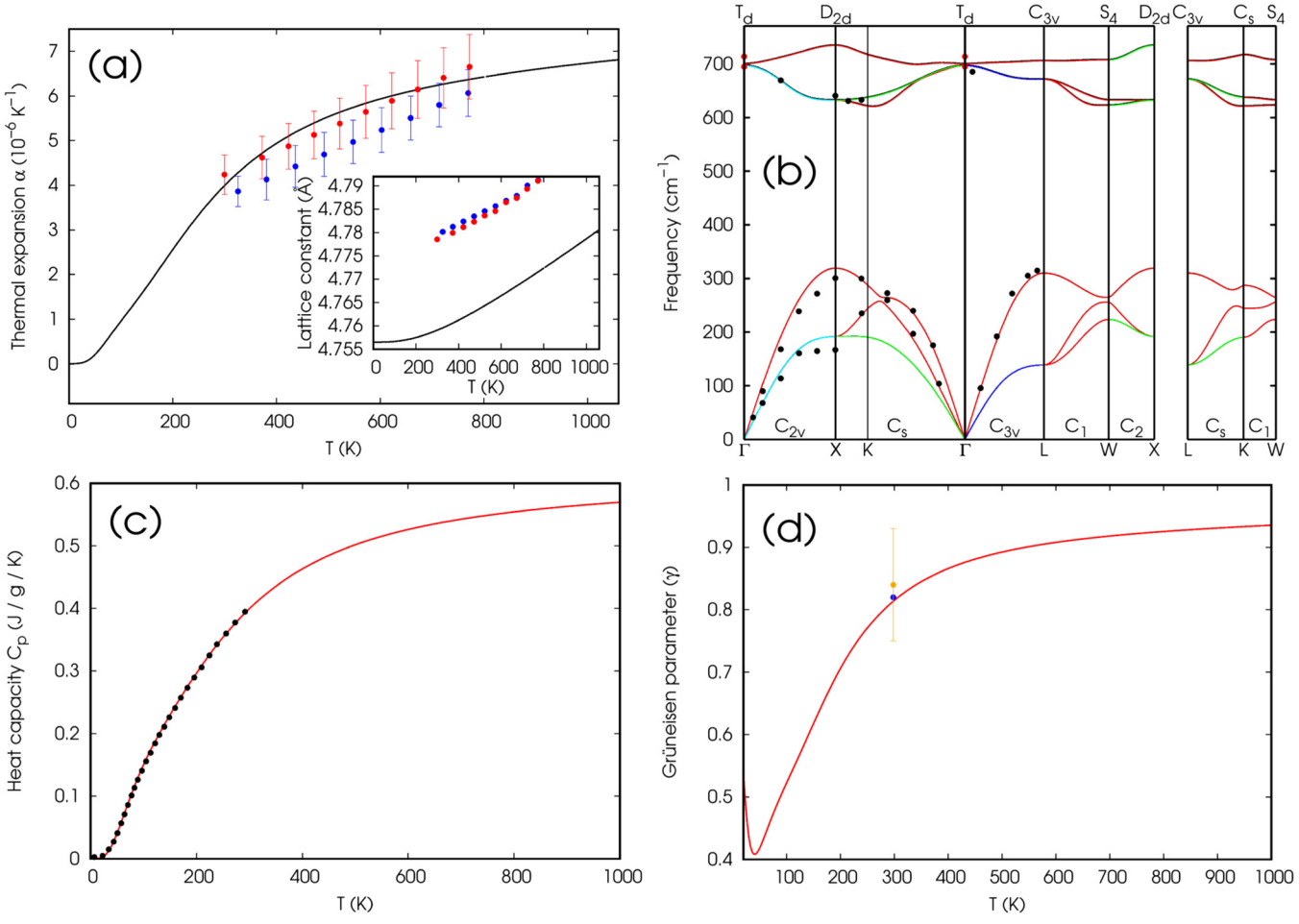

FIG. 3. (a) Thermal expansion and temperature dependence of the lattice parameter (inset). Black lines represent this work; the points are experimental data: blue[6] and red.[7] (b) Phonon dispersion curves at $T = 300$ K (colored lines) and experimental points: black[25] and red.[26] The colors of the phonon branches indicate their symmetry (as explained in the thermo_pw documentation). Phonon curves at $T = 0$ K (black lines, barely visible only in the optical branches). (c) Computed isobaric heat capacity (red line) and comparison with the experimental one (points) adapted from Chen *et al.*[7] (d) Average Grüneisen parameter. This work (red curve) and experimental points: blue[6] and orange.[7]

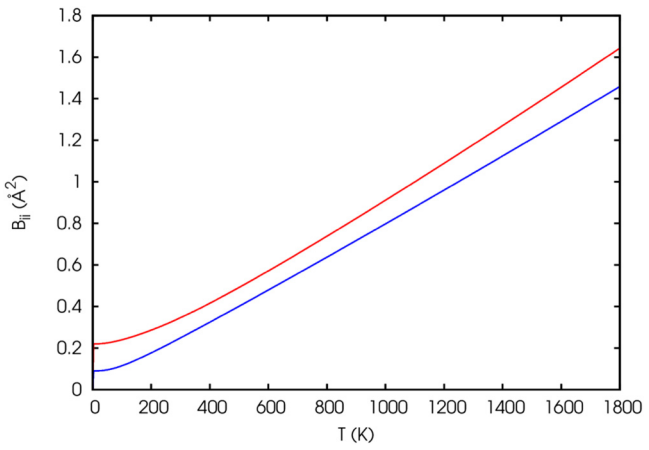

FIG. 4. Temperature dependent atomic B-factor for the cubic BAs: boron (red) and arsenic (blue).

Finally, in Fig. 4, we show our estimate of the BF for boron (red) and arsenic (blue). The BF of boron is 0.35 Å^2 at $T = 300$ K and grows up to 0.74 Å^2 at $T = 800$ K. The BF of arsenic is smaller because of the larger mass: 0.25 Å^2 at $T = 300$ K and 0.64 Å^2 at $T = 800$ K. They are smaller than the BFs of silicon,[17] which has 0.52 Å^2 at $T = 300$ K and 1.29 Å^2 at $T = 800$ K.

V. CONCLUSIONS

We studied TDECs of BAs by means of *ab initio* simulation by using the recent tools implemented in the thermo_pw code within the QHA. The values of the adiabatic ECs at $T = 300$ K are $C_{11} = 2807$ kbar, $C_{12} = 754$ kbar and $C_{44} = 1507$ kbar. We found that in the temperature range 0−1800 K, the percentage softening of the adiabatic ECs is approximately 11% for C_{11}, approximately 9% for C_{12}, and approximately 13% for C_{44}. The order of magnitude of the softening is consistent with the temperature variation of the longitudinal sound velocity measured along the [111] direction.[6] The slope of the curves is different below RT and similar for larger temperatures. The softening computed in BAs is slightly smaller than that calculated for silicon in the temperature range 0–800 K.[13] We also computed thermodynamic properties of BAs such as the TE, the heat capacity, and the average Grüneisen parameter, finding good agreement with experiments. Finally, we presented the calculated atomic BFs as a function of the temperature for which no information, neither experimental nor theoretical, has been available so far.

ACKNOWLEDGMENTS

Computational facilities have been provided by SISSA through its Linux Cluster and ITCS and by CINECA through the SISSA-CINECA 2019-2020 Agreement.

DATA AVAILABILITY

The data that support the findings of this study are available within the article.

REFERENCES

[1]J. S. Kang, H. Wu, and Y. Hu, Nano Lett. **17**, 7507 (2017).
[2]J. S. Kang, M. Li, H. Wu, H. Nguyen, and Y. Hu, Science **361**, 575 (2018).
[3]S. Li, Q. Zheng, Y. Lv, X. Liu, X. Wang, P. Y. Huang, D. G. Cahill, and B. Lv, Science **361**, 579 (2018).
[4]F. Tian, B. Song, X. Chen, N. K. Ravichandran, Y. Lv, K. Chen, S. Sullivan, and J. Kim, Science **361**, 582 (2018).
[5]F. Tian, K. Luo, C. Xie, B. Liu, X. Liang, L. Wang, G. A. Gamage, H. Sun, H. Ziyaee, J. Sun, Z. Zhao, B. Xu, G. Gao, X.-F. Zhou, and Z. Ren, Appl. Phys. Lett. **114**, 131903 (2019).
[6]J. S. Kang, M. Li, H. Wu, H. Nguyen, and Y. Hu, Appl. Phys. Lett. **115**, 122103 (2019).
[7]X. Chen, C. Li, F. Tian, G. A. Gamage, S. Sullivan, J. Zhou, D. Broido, Z. Ren, and L. Shi, "Thermal expansion coefficient and lattice anharmonicity of cubic boron arsenide," Phys. Rev. Appl. **11**, 064070 (2019).
[8]S. Q. Wang and H. Q. Ye, Phys. Status Solidi B **240**, 45 (2003).
[9]F. E. H. Hassan, H. Akbarzadeh, and M. Zoaeter, J. Phys. Condens. Matter **16**, 293 (2004).
[10]H. Meradji, S. Drablia, S. Ghemid, H. Belkhir, B. Bouhafs, and A. Tadjer, Phys. Status Solidi B **241**, 2881 (2004).
[11]L. Bing, L. R. Feng, and Y. X. Dong, Chin. Phys. B **19**, 076201 (2010).
[12]S. Daoud, N. Bioud, and N. Bouarissa, Mater. Sci. Semicond. Process. **31**, 124 (2015).
[13]C. Malica and A. Dal Corso, J. Phys. Condens. Matter **32**, 315902 (2020).
[14]J. F. Nye, *Physical Properties of Crystals* (Oxford Science Publications, 1985).
[15]M. Palumbo and A. Dal Corso, J. Phys. Condens. Matter **29**, 395401 (2017).
[16]M. Palumbo and A. Dal Corso, Phys. Status Solidi B **254**, 1700101 (2017).
[17]C. Malica and A. Dal Corso, Acta Crystallogr. Sect. A **75**, 624 (2019).
[18]P. Giannozzi, S. Baroni, N. Bonini, M. Calandra, R. Car, C. Cavazzoni, D. Ceresoli, G. L. Chiarotti, M. Cococcioni, I. Dabo, A. Dal Corso, S. De Gironcoli, S. Fabris, G. Fratesi, U. G. Ralph Gebauer, C. Gougoussis, A. Kokalj, M. Lazzeri, L. Martin-Samos, N. Marzari, F. Mauri, R. Mazzarello, S. Paolini, A. Pasquarello, L. Paulatto, C. Sbraccia, S. Scandolo, G. Sclauzero, A. P. Seitsonen, A. Smogunov, P. Umari, and R. M. Wentzcovitch, J. Phys. Condens. Matter **21**, 395502 (2009).
[19]P. Giannozzi, O. Andreussi, T. Brumme, O. Bunau, M. B. Nardelli, M. Calandra, R. Car, C. Cavazzoni, D. Ceresoli, M. Cococcioni, N. Colonna, I. Carnimeo, A. Dal Corso, S. De Gironcoli, P. Delugas, R. A. DiStasio, A. Ferretti, A. Floris, G. Fratesi, G. Fugallo, R. Gebauer, U. Gerstmann, F. Giustino, T. Gorni, J. Jia, M. Kawamura, H.-Y. Ko, A. Kokalj, E. Küçükbenli, M. Lazzeri, M. Marsili, N. Marzari, F. Mauri, N. L. Nguyen, H.-V. Nguyen, A. O. de-la Roza, L. Paulatto, S. Poncé, D. Rocca, R. Sabatini, B. Santra, M. Schlipf, A. P. Seitsonen, A. Smogunov, I. Timrov, T. Thonhauser, P. Umari, N. Vast, X. Wu, and S. Baroni, "Advanced capabilities for materials modelling with quantum ESPRESSO," J. Phys. Condens. Matter **29**, 465901 (2017).
[20]See https://dalcorso.github.io/thermo_pw for information about the `thermo_pw` software.
[21]P. E. Blöchl, Phys. Rev. B **50**, 17953 (1994).
[22]See https://github.com/dalcorso/pslibrary for information about the `pslibrary` pseudopotentials library.
[23]S. Baroni, S. de Gironcoli, A. Dal Corso, and P. Giannozzi, Rev. Mod. Phys. **73**, 515 (2001).
[24]A. Dal Corso, Phys. Rev. B **82**, 075123 (2010).
[25]H. Ma, C. Li, S. Tang, J. Yan, A. Alatas, L. Lindsay, B. C. Sales, and Z. Tian, Phys. Rev. B **94**, 220303 (2016).
[26]R. G. Greene, H. Luo, and A. L. Ruoff, Phys. Rev. Lett. **73**, 2476 (1994).
[27]C. Kittel, *Introduction to Solid State Physics* (Wiley, New York, 1976).
[28]D. A. Broido, L. Lindsay, and T. L. Reinecke, Phys. Rev. B **88**, 214303 (2013).
[29]F. Benkabou, C. Chikr.Z, H. Aourag, P. J. Becker, and M. Certier, Phys. Lett. A **252**, 71 (1999).
[30]S. Daoud, N. Bioud, and N. Lebga, Chin. J. Phys. **57**, 165 (2019).